A method for estimating optical properties of dusty cloud

Tianhe Wang (王天河)[1,2] and Jianping Huang (黄建平)[1*]

[1]*Key Laboratory for Semi-Arid Climate Change of the Ministry of Education, College of Atmospheric Sciences, Lanzhou University, Lanzhou 730000, China*

[2]*Institute of Atmospheric Physics, Chinese Academy of Sciences, Beijing 100029, China*

[*]*E-mail: hjp@lzu.edu.cn*

Received February 12, 2009

Based on the scattering properties of nonspherical dust aerosol, a new method is developed for retrieving dust aerosol optical depths of dusty clouds. The dusty clouds are defined as the hybrid system of dust plume and cloud. The new method is based on transmittance measurements from surface-based instruments multi-filter rotating shadowband radiometer (MFRSR) and cloud parameters from lidar measurements. It uses the difference of absorption between dust aerosols and water droplets for distinguishing and estimating the optical properties of dusts and clouds, respectively. This new retrieval method is not sensitive to the retrieval error of cloud properties and the maximum absolute deviations of dust aerosol and total optical depths for thin dusty cloud retrieval algorithm are only 0.056 and 0.1, respectively, for given possible uncertainties. The retrieval error for thick dusty cloud mainly depends on lidar-based total dusty cloud properties.

OCIS codes: 010.0280, 010.1100, 280.1100.

doi: 10.3788/COL20090705.0368.

Tropospheric aerosols are known to play an important role in terrestrial climate system, and yet thought to be a source of significant uncertainties in studies of the Earth's climate and climate change. It is because that aerosols can not only directly reflect and absorb the incoming solar radiation (direct effect) but also indirectly increase cloud albedo and suppress precipitation by modifying the cloud microphysical properties (indirect effect)[1,2]. Furthermore, absorbing aerosols, such as black carbon and mineral dust, could contribute to high adiabatic heating in the atmosphere that often enhances cloud evaporation (semi-direct effect)[3,4]. The total aerosol direct and indirect effets on the cloud albedo radiative forcing relative to the start of the industrial era have a larger cooling effect on the climate system, which are estimated to be at the ranges of $[-0.9, -0.1]$ and $[-1.8, -0.3]$ W/m^2, respectively, as derived from models and observations[5]. Narrowing this huge uncertainty is an outstanding issue, which has been approached by relating satellite observed cloud properties and aerosols to each other[6]. However, the degree of mixture of aerosol and cloud particles is a big uncertainty. So far, there is not proper method to estimate optical properties of such mixture clouds. To deeply understand and accurately quantify both the aerosol direct and indirect radiative forcing effects, a retrieval method for estimating their optical properties in the mixture of aerosol and cloud particles is needed urgently.

Dust is one the of important aerosol types in East Asia due to the frequently occurrence of dust storms from Taklamakan Desert of China and the Gobi Desert of Mongolia in recent years[7]. The dust layers associated with these storms often travel thousands of kilometers at high altitudes, moving from the continent to the open sea near Korea and Japan[8−10], which may have serious impact on the global climate system. Asian dust may also have a significant effect on the atmospheric radiation budget because of large emission amount. The annual mean dust emission from China is estimated to be around 800 teragrams (Tg)[11]. And thus more and more attentions have been focused on the climate and radiative impact of dust aerosols[8,12−14]. Furthermore, cloud optical properties over northwestern China have been analyzed statistically[15]. The cloud and dust plume hybrid system (named as dusty cloud) will be a popular phenomenon. Additionally, the facts of Asian dust aerosol indirect and semi-direct effects have been confirmed through satellite observation[4,7] and numerical model[16]. It will be helpful to check up the practicability and accuracy of this retrieval method, and at the same time, many parameters of Asian dust aerosol optical properties used in this method will be obtained easily.

Irregular shapes of Asian dust aerosol have been revealed by *in situ* measurements[17,18]. Kalashnikova *et al.* showed that nonspherical dust particles had substantially different scattering phase functions, asymmetry factors, optical depths, and single-scattering albedos, as compared with those of the volume-equivalent[19]. Dubovik *et al.* also showed that neglecting the asphericity of dust particles could lead to incorrect results in retrieving dust properties (e.g., size distribution and refractive index) from radiometric measurements[20]. Therefore, in this letter, we focus on the nonspherical effect of Asian dust aerosols. Meanwhile, we develop an algorithm for retrieving dust aerosol optical properties in the mixture of dust and cloud particles based on the combination of surface-based multi-filter rotating shadowband radiometer (MFRSR) and lidar measurements.

In order to reduce the effect of irregular shape, we adopt the first-order approximation of nonspherical dust particles, spheroids. The combination method of T-matrix[21] and improved geometric optics method (IGOM)[22], developed by Yang *et al.*[23], is employed to calculate single-scattering properties of individual dust particls. The boundary size parameter is set as 40 for calculation time consideration, i.e., T-matrix is employed for size parameters less than 40 and IGOM for larger. The single-scattering properties of dust particles are sensitive to aspect ratio and refractive index of these particles. In this study, the aspect ratios of dust particles are assumed to be 1.7, the refractive index is assumed as 1.41+0.003i, according to the average of *in situ* data at 440 nm at five Aerosol Robotic Network (AERONET) Chinese sites during dusty days from 2001 to 2005[24].

The scattering properties for the dust particle population are defined by integrating the single particles over the following bimodal lognormal size distribution:

$$\frac{\mathrm{d}N}{\mathrm{d}\ \ln\ r}=\sum_{i=1}^{2}\left\{\frac{N_i}{\sqrt{2\pi}\ln\ \sigma_i}\exp\left[-\frac{(\ln r-\ln r_{\mathrm{g},i})^2}{2\ln^2\sigma_i}\right]\right\}, \quad (1)$$

where N is the total number density of dust aerosol, r is the radius of dust aerosol, $r_{\mathrm{g},i}$ and σ_i are the mean geometric radius and standard deviation at mode i, respectively, N_i is number density of dust aerosol at mode i, here we assume that the distribution is normalized ($\sum_{i=1}^{2} N_i = 1$). These parameters are converted from that of CALIPSO dust aerosol volume size distribution model at desert regions or close to deserts[25] by $r_{\mathrm{g},i} = r_{\mathrm{v},i}\exp(-3\ln^2\sigma_i)$[26], where $r_{\mathrm{v},i}$ is the geometric radius of volume size distribution. The calculated single-scattering albedo, asymmetry factor, and effective radius of Asian dust aerosols are 0.934, 0.680, and 0.387 μm, respectively. They are very close to the average results at 10 Asian AERONET sites during dusty days from 2001 to 2005 analyzed by Yu *et al.*, who also concluded that single-scattering albedo and asymmetry factor of Asian dust could be used as 0.94 and 0.67 over the dust source region of China, respectively[24]. It means that the selected dust model can stand for the true dust aerosol size distribution over Asian dust source regions.

The surface-based radiation instrument, MFRSR, is employed for our retrieval method. MFRSR is a seven-channel radiometer with six passbands of 10-nm full-width at half-maximum (FWHM) nominally centered at 415, 500, 610, 665, 860, and 940 nm, and an unfiltered silicon pyranometer[27]. It allows the accurate determination of atmospheric transmittances at each passband without requiring absolute calibration because it measures both total (global) horizontal irradiance and direct-normal irradiance using the same detectors by a blocking technique. Langley regression of the direct-normal irradiance taken on stable clear days can be used to extrapolate the instrument's response to the top of the atmosphere, and this calibration can then be applied to the total horizontal irradiance in cloud periods. Transmittances are calculated subsequently under cloudy conditions as the ratio of the uncalibrated MFRSR signal to the extrapolated top-of-atmosphere value.

Furthermore, a family of retrieval algorithms has been developed for inferring cloud optical properties from MFRSR combined with microwave radiometer[28]. Cloud optical depth and effective radius can be simultaneously retrieved through the use of a nonlinear least-square minimization in conjunction with an adjoint method of radiative transfer. These retrieval algorithms have been extensively tested and validated, demonstrating good accuracies[29,30]. Based on the combination of above existing algorithms, Wang *et al.* developed an algorithm to retrieve optical properties of mixed-phase and thin cloud, the mixture of water droplets and ice crystals[31]. One can take advantage of simultaneous spectral measurements of direct-beam and total radiation from MFRSR and utilize the difference of scattering phase function of ice and liquid clouds on the partition of direct and total radiation to derive cloud thermodynamic phase information and mix ratio, and consequently to accurately infer optical depths of optically thin clouds. The algorithm is simplified only by the simple linear combination of retrievals for pure water and ice cloud conditions. Therefore, the algorithm could be applicable to the mixture of two media, such as dusty cloud.

Figure 1 shows the comparison of phase functions at 415 nm for water clouds with effective radii of 4, 8, and 12 μm and Asian dust aerosols. Water clouds have stronger forward scattering in the forward scattering lobe (scattering angle < 10°, shown in Fig. 1(b)) than dust aerosols. It is clearly evident that the loading amount of dust and cloud is a major factor in determining between direct-beam and total radiation, while effective particle sizes of clouds within the same cloud phase play a minor role. Those insights lay the foundation for our proposed retrieval algorithm.

The direct beam and total transmittances observed by MFRSR at given dust aerosol and cloud optical depths, τ_{dust} and τ_{cloud}, and effective radius R_{e}, can be described as

$$\begin{aligned} I^{\mathrm{dir}} \quad & (\mu_0, \tau_{\mathrm{bkg}}, \tau_{\mathrm{dust}}, \tau_{\mathrm{cloud}}, R_{\mathrm{e}}) \\ & = \exp[-(\tau_{\mathrm{ray}} + \tau_{\mathrm{bkg}} + \tau_{\mathrm{dust}} + \tau_{\mathrm{cloud}})/\mu_0] \\ & +(B_0 - B_9), \\ I^{\mathrm{tot}} \quad & (\mu_0, \tau_{\mathrm{bkg}}, \tau_{\mathrm{dust}}, \tau_{\mathrm{cloud}}, R_{\mathrm{e}}) \\ & = \mu_0 I^{\mathrm{dir}}(\mu_0, \tau_{\mathrm{bkg}}, \tau_{\mathrm{dust}}, \tau_{\mathrm{cloud}}, R_{\mathrm{e}}) \\ & +I^{\mathrm{dif}}(\mu_0, \tau_{\mathrm{bkg}}, \tau_{\mathrm{dust}}, \tau_{\mathrm{cloud}}, R_{\mathrm{e}}), \end{aligned} \quad (2)$$

where I^{dir}, I^{dif}, and I^{tot} are the transmittances of direct normal, diffuse horizontal, and total horizontal at the cosine of solar zenith angle μ_0, respectively. Here τ_{ray}

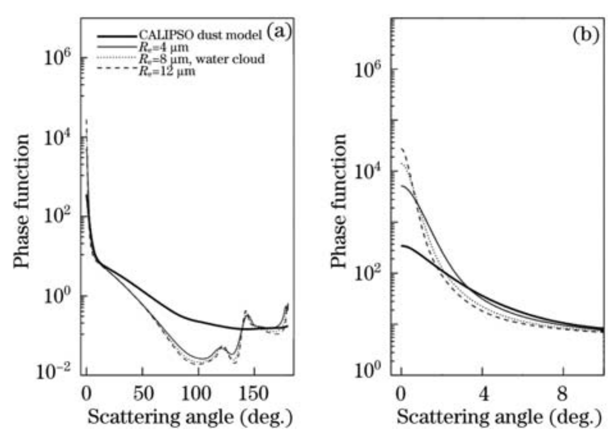

Fig. 1. Comparison of phase function at 415 nm between spheroidal dust aerosol and spherical water clouds with different radii. (b) Expansion of (a) for a scattering angle range of 0° − 10°.

and $\tau_{\rm bkg}$ are optical depths of Rayleigh scattering and background aerosols, respectively, and B_0 and B_9 are the blocked scattering radiation into the field of view (FOV) at two block angles, 0° and 9°, respectively. $B_0 - B_9$ stands for the forward-scattering radiation presumed by the MFRSR as the direct radiation. We use the modified discrete ordinate radiative transfer (DISORT) to accurately and rapidly compute the forward direct radiance and total radiation[32,33]. The total radiation is influenced strongly by surface albedo and atmospheric absorptions, therefore, the 415-nm channel will be selected in our retrieval. It keeps the surface albedo relatively constant when snow is absent and avoids all gaseous absorption, except for NO_2, which has negligible impact under normal conditions.

However, the algorithm is only applicable to the mixture of two thinner media (optical depth < 10 or much less). When these optical depths thicken, the direct irradiation decreases and even to zero, the only total (diffuse) transmittance can be applicable to our retrieval. It is impossible to derive their optical depths in a single function with two unknown parameters, such as $\tau_{\rm dust}$ and $\tau_{\rm cloud}$ for dusty cloud. In this case, we have to employ other instrumental measurements to extend the algorithm for more situations. The cloud products from the moderate resolution imaging spectroradiometer (MODIS) are widely accepted as the state-of-the-art by the meteorological community, but are not available at a regular temporal frequency over one specific region due to the polar orbiting nature of the instrument. Near-real-time cloud products retrieved from the geostationary satellite flying on the Asian region such as FY-2C and MTSAT-1R could satisfy our research, but lower temporal resolution and temporal-spatial mismatch could be big error source in radiation closure and actual retrieval. Therefore, surface-based lidar active measurements can be employed in our retrieval algorithm for more accurate total dusty cloud optical properties[34,35]. Dusty clouds currently cannot be distinguished and thus the error of cloud properties retrieval is increased. For simplicity, we assume the error as uncertainty of lidar retrieval algorithm. Herein, one unknown parameter $\tau_{\rm dust}$ in Eq. (2) will be calculated.

To illustrate the sensitivity of total transmittance to cloud particle size and dust aerosol loading, the MFRSR measurements are simulated for mixtures of water clouds and dust aerosols. The effective radii for water clouds are assumed to be ranging from 4 to 16 μm. Optical depths for water clouds and dust are assumed to be ranging from 0 to 32 and from 0 to 1.8, respectively. Water cloud and dust layer are assumed to locate at $1 - 2$ km altitude. Here we assume linearly weighted optical properties by optical depths of water clouds and dust as optical properties of dusty clouds, despite optical properties of some dust particles coating water droplets have been changed.

Figure 2 shows the direct and total transmittances as functions of total optical depths for dusty clouds with solar zenith angle of 25° and water cloud effective radius of 8 μm at 415-nm wavelength. Obviously, changes of dust loading will lead to significant changes of total transmittance, which is mainly due to the stronger absorption of dust than water cloud droplets. Therefore, transmittances of dusty cloud cannot be simplified by pure dust aerosol and water cloud conditions as thin and mixed-phase cloud.

To cover all kinds of dusty cloud conditions, a method is developed and a schematic view is outlined in Fig. 3. For thin dusty clouds, under the assumption of radiation closure, the optical depth retrieved from direct transmittance is equal to that from total transmittance. Therefore, for the measurements of MFRSR, we have

$$e^{\rm dir} = I^{\rm dir}_{\rm obs} - I^{\rm dir}_{\rm sim}(\mu_0, \tau_{\rm bkg}, \tau_{\rm dust}, \tau_{\rm cloud}, R_{\rm e}),$$
$$e^{\rm tot} = I^{\rm tot}_{\rm obs} - I^{\rm tot}_{\rm sim}(\mu_0, \tau_{\rm bkg}, \tau_{\rm dust}, \tau_{\rm cloud}, R_{\rm e}), \quad (3)$$

where $I^{\rm dir}_{\rm obs}(I^{\rm tot}_{\rm obs})$ and $I^{\rm dir}_{\rm sim}(I^{\rm tot}_{\rm sim})$ are measured and simulated direct (total) transmittances, $e^{\rm dir}$ and $e^{\rm tot}$ are errors between them, respectively. If present, values from other measurements will be used for effective radius, otherwise, a climatological value of 8 μm is assumed. The optical depth of dust aerosol and water cloud can be evaluated as the least-square minimum of the difference between the measured and simulated transmittances in the above equations. However, for thick dusty clouds ($I^{\rm dir}_{\rm obs} \approx 0$), only the total transmittance is available. According to Eq. (3), optical depths of dust aerosol can be derived by iterative calculation till $e^{\rm tot} = 0$ when lidar-based cloud optical depth is available. On the basis of experience from MFRSR, the accuracy of the solar constant at a nongaseous absorption passband from the Langley regression calibration is within 1%[36]. Therefore, in the following tests we set a random measurement error of 1%.

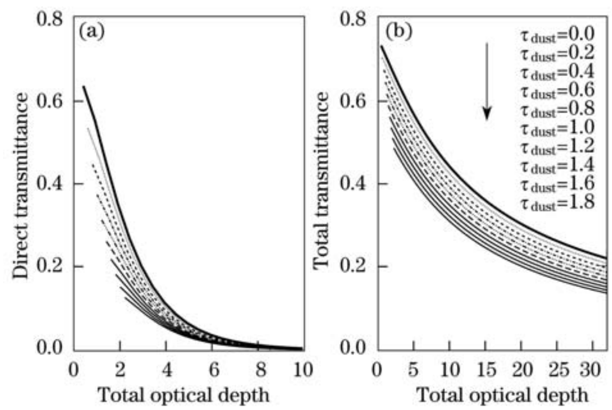

Fig. 2. Simulated (a) direct and (b) total transmittances as functions of total optical depth for dusty cloud given dust aerosol optical depth ranging from 0 to 1.8 with solar zenith angle 25° and water cloud droplets effective radius of 8 μm at 415-nm wavelength.

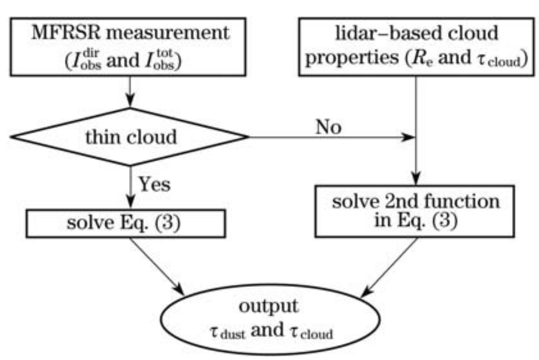

Fig. 3. Schematic of retrieval method for dusty clouds.

To simulate real dusty cloud scenes and test for a large range of conditions, we set up 100 random cases as our basic test in thin and thick dusty clouds, respectively. In thin dusty cloud cases, in order to remove the cases with extremely small direct transmittance, the solar zenith angle changes from 25° to 55°, the dust and total dusty cloud optical depths are randomly selected from 0.2 to 1.8 and from 2.5 to 8, respectively. The comparisons between input (true) and retrieved dust and total optical depths with a random error of 1% in radiometric error, 10% and 15% in effective radius are shown in Figs. 4(a) and (b), respectively. The maximum absolute deviations (relative errors) of dust and total optical depths are only 0.056 (15%, most cases under 8%) and 0.1 (8%) for all cases with 1% radiometric error, respectively, 0.014 (7.6%) and 0.012 (0.6%) with 10% and 15% effective radius errors. It illustrates that this new retrieval method for thin dusty cloud is not sensitive to MFRSR measurements and assumption of R_e. For thick dusty clouds, the comparison of dust optical depth is shown in Figs. 4(c) and (d) with the same conditions as thin dusty clouds except for solar zenith angle expanding from 25° to 70° and total dusty cloud optical depth from 2.5 to 30. The maximum absolute deviations (relative errors) are also only 0.031 (13.8%) with 1% radiometric error and 0.031 (15.3%) with 10% and 15% effective radius errors. Obviously, the retrieval error is very small from Langley regression correction for MFRSR measurements and the assumption of R_e whatever in thin or thick dusty cloud retrieval. It also represents the powerful ability of this algorithm for dusty cloud retrieval. Furthermore, it is worth noting that the error of total optical depth from lidar may be an important impact factor for thick dusty cloud retrieval and cannot be ignored. But it depends on the accuracy of lidar cloud retrieval algorithm, and thus here we do not discuss more about it due to its complexity.

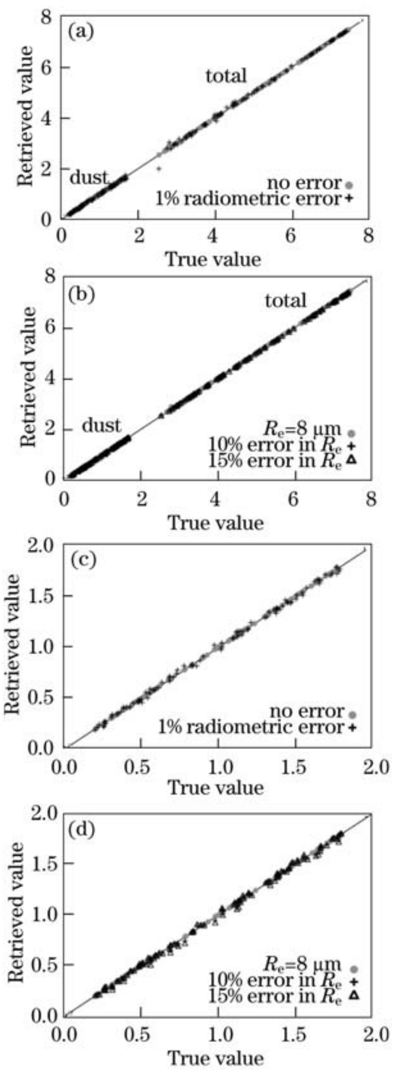

Fig. 4. Comparisons between input (true) and retrieved dust and total optical depths from thin dusty cloud retrieval algorithm for 100 random cases with random errors of (a) 1% in radiometric error and (b) 10% and 15% in effective radius. (c), (d): True and retrieved dust optical depths from thick dusty cloud retrieval algorithm with random errors.

Dusty cloud, a kind of universal atmosphere phenomena at desert source region, can be observed by surface/satellite-based instruments. However, their optical properties and radiative effects have big uncertainty. The proposed retrieval method allows distinguishing and estimating the optical properties of dusts and clouds in the mixture of pure dust aerosols and pure water clouds. It will give us a possibility to directly evaluate the aerosol direct and indirect effects. The combination of surface-based instruments will increase the power of detecting aerosol radiative effects. Furthermore, the retrieval method may be applied to other more routine radiation instruments. However, the practicability and accuracy of this retrieval method still need to be checked up by more actual *in situ* measurements.

This work was supported by the Knowledge Innovation Program of the Chinese Academy of Sciences (No. IAP09311) and the National Natural Science Foundation of China (Nos. 40725015 and 40633017). We thank Dr. Ping Yang for providing IGOM codes.

References

1. S. Twomey, J. Atmos. Sci. **34,** 1149 (1977).
2. B. A. Albrecht, Science **245,** 1227 (1989).
3. A. S. Ackerman, O. B. Toon, D. E. Stevens, A. J. Heymsfield, V. Ramanathan, and E. J. Welton, Science **288,** 1042 (2000).
4. J. Huang, B. Lin, P. Minnis, T. Wang, X. Wang, Y. Hu, Y. Yi, and J. K. Ayers, Geophys. Res. Lett. **33,** L19802 (2006).
5. P. Forster, V. Ramaswamy, P. Artaxo, T. Berntsen, R. Betts, D. W. Fahey, J. Haywood, J. Lean, D. C. Lowe, G. Myhre, J. Nganga, R. Prinn, G. Raga, M. Schulz, and R. Van Dorland, in *Climate Change 2007: The Physical Science Basis. Contribution of Working Group I to the Fourth Assessment Report of the Intergovernmental Panel on Climate change* S. Solomon, D. Qin, M. Manning, Z. Chen, M. Marquis, K. B. Averyt, M. Tignor, and H. L. Miller, (eds.) (Cambridge University Press, Cambridge and New York, 2007).
6. G. Feingold, L. A. Remer, J. Ramaprasad, and Y. J. Kaufman, J. Geophys. Res. **106,** 22907 (2001).
7. J. Huang, P. Minnis, B. Lin, T. Wang, Y. Yi, Y. Hu, S. Sun-Mack, and K. Ayers, Geophys. Res. Lett. **33,** L06824 (2006).
8. J. Huang, P. Minnis, B. Chen, Z. Huang, Z. Liu, Q. Zhao,

Y. Yi, and J. K. Ayers, J. Geophys. Res. **113,** D23212 (2008).
9. T. Takemura, I. Uno, T. Nakajima, A. Higurashi, and I. Sano, Geophys. Res. Lett. **29,** 2158 (2002).
10. J. M. Haywood, V. Ramaswamy, and B. J. Soden, Science **283,** 1299 (1999).
11. Z. Li, "Aerosol and climate: a perspective over East Asia" in *Observation, Theory and Modeling of Atmospheric Variability* X. Zhu, (ed.) (World Scientific, Singapore, 2004) pp.501−525.
12. J. Huang, J. Ge, and F. Weng, Remote Sens. Environ. **110,** 186 (2007).
13. J. Huang, Y. Wang, T. Wang, and Y. Yi, Prog. Nat. Sci. **16,** 1084 (2006).
14. J. Ge, J. Huang, F. Weng, and W. Sun, Atmos. Chem. Phys. **8,** 4903 (2008).
15. Y. Chen, H. Bai, J. Huang, H. Zhang, J. Ge, X. Guan, and X. Mao, Chin. Opt. Lett. **6,** 454 (2008).
16. Y. Yin and L. Chen, Atmos. Chem. Phys. **7,** 3497 (2007).
17. K. Okada, J. Heintzenberg, K. Kai, and Y. Qin, Geophys. Res. Lett. **28,** 3123 (2001).
18. Y. Gao and J. R. Anderson, J. Geophys. Res. **106,** 18037 (2001).
19. O. V. Kalashnikova and I. N. Sokolik, J. Quant. Spectrosc. Rad. Transfer **87,** 137 (2004).
20. O. Dubovik, A. Sinyuk, T. Lapyonok, B. N. Holben, M. Mishchenko, P. Yang, T. F. Eck, H. Volten, O. Muñoz, B. Veihelmann, W. J. van der Zande, J.-F. Leon, M. Sorokin, and I. Slutsker, J. Geophys. Res. **111,** D11208 (2006).
21. M. I. Mishchenko and L. D. Travis, Appl. Opt. **33,** 7206 (1994).
22. P. Yang and K. N. Liou, Appl. Opt. **35,** 6568 (1996).
23. P. Yang, Q. Feng, G. Hong, G. W. Kattawar, W. J. Wiscombe, M. I. Mishchenko, O. Dubovik, I. Laszlo, and I. N. Sokolik, J. Aerosol Science **38,** 995 (2007).
24. X. Yu, T. Cheng, J. Chen, and Y. Liu, Atmos. Environ. **40,** 5787 (2006).
25. A. H. Omar, D. Winker, and J.-G. Won, Proc. SPIE **5240,** 153 (2004).
26. R. C. Levy, L. A. Remer, S. Mattoo, E. F. Vermote, and Y. J. Kaufman, J. Geophys. Res. **112,** D13211 (2007).
27. L. Harrison, J. Michalsky, and J. Berndt, Appl. Opt. **33,** 5118 (1994).
28. Q. Min and L. C. Harrison, Geophys. Res. Lett. **23,** 1641 (1996).
29. Q.-L. Min, M. Duan, and R. Marchand, J. Geophys. Res. **108,** 4547 (2003).
30. Q. Min, P. Minnis, and M. M. Khaiyer, J. Geophys. Res. **109,** D15207 (2004).
31. T. Wang and Q. Min, J. Geophys. Res. **113,** D19203 (2008).
32. Q. Min, E. Joseph, and M. Duan, J. Geophys. Res. **109,** D02201 (2004).
33. M. Duan and D. Lü, J. Remote Sens. (in Chinese) **11,** 359 (2007).
34. J. Qiu, Advances Atmos. Sci. **12,** 177 (1995).
35. Z. Wang, R. Chi, B. Liu, and J. Zhou, Chin. Opt. Lett. **6,** 235 (2008).
36. J. J. Michalsky, J. A. Schlemmer, W. E. Berkheiser, J. L. Berndt, L. C. Harrison, N. S. Laulainen, N. R. Larson, and J. C. Barnard, J. Geophys. Res. **106,** 12099 (2001).